Initiation and runout characteristics of partially saturated debris flows in Ohya landslide scar, Japan

Fumitoshi Imaizumi[1*], *Shunsuke* Oya[2], and *Shoki* Takayama[1]

[1]Faculty of Agriculture, Shizuoka University, Shizuoka, Japan
[2] Nippon Koei Co., Ltd. Fukuoka, Japan

Abstract. A partially saturated flow, which has an unsaturated layer in its upper part, has been monitored in the steep initiation zones of debris flows. Understanding the initiation and runout characteristics of partially saturated flows is essential for predicting the timing and magnitude of downstream debris flows. Monitoring performed using time-lapse cameras and water pressure sensors in the Ohya landslide scar in central Japan allowed us to obtain data on a series of partially saturated debris flow surges from initiation to termination on July 6, 2020, and July 13, 2021. Debris flow surges were mainly induced by repetitive mass movement of sediment deposit caused by the overland flow erosion of channel deposits, channel deposit slides, and water and sediment supply from channel banks and tributaries. The excess pore water pressure in a partially saturated flow on July 6, 2020, was clearly higher than that on July 13, 2021. Rainfall patterns, which control the water content in channel deposits, and the flow height likely affect the magnitude of the excess pore water pressure in partially saturated flows.

1 Introduction

Partially saturated debris flows, which have an unsaturated layer in their upper part, have been monitored in many debris flow torrents worldwide [1-3]. Partially saturated flow is typical in steep debris-flow initiation zones due to the higher shear stress at the bottom of a sediment mass, which exceeds the shear strength even without full saturation of the sediment mass [4]. Many debris flow monitoring activities have been undertaken in debris flow transportation zones, in which fully saturated flow is the predominant flow type. Therefore, initiation and runout characteristics of partially saturated flows remain unclear.

Debris flows with higher pore water pressure have high flow mobility and a long travel distance due to the decreased flow resistance caused by a reduction in the effective stress among large particles [5]. Pore water pressure consists of hydrostatic and excess pore water pressures [6], and excess pore water pressure occurs owing to contraction by surrounding large particles under high shear stress [5], loading of particles to the interstitial water [7], and Reynolds stress from the turbulence of the interstitial water [8]. Many of these findings have been obtained through experiments on fully saturated debris flows. Excess pore water pressure in a partially saturated flow is yet to be understood.

The aim of this study was to elucidate the initiation and runout characteristics of partially saturated debris flows based on field monitoring of the Ohya landslide scar in central Japan. Debris flows occur frequently in the Ohya landslide due to the mobilization of deposits (e.g., channel deposits and talus slopes) during rainfall events. We monitored debris flows from initiation to termination using time-lapse cameras (TLCs) on July 6, 2020, and July 13, 2021. The pore water pressure in the debris flows was measured using water-pressure sensors. The objectives of this study were to (1) clarify the initiation timing, location, and mechanism of partially saturated flows; (2) reveal the runout characteristics of partially saturated flows; and (3) discuss the factors affecting pore water pressure in partially saturated flows.

2 Study site

The Ohya landslide, which has a total volume of 120 million m^3, was initiated during an earthquake in 1707 CE. Most of debris flow in Ohya landslide occurs in Ichinosawa torrent, which flows down from the northern end of the landslide (Fig. 1). The Ichinosawa catchment has an altitude ranging between 1,270 and 1,905 m a.s.l. with an area of 0.3 km^2, and channel length of 1000 m. It is divided into upper and lower Ichinosawa, separated by the “Ohya-ohtaki” waterfall located at 1,450 m a.s.l. (P20 in Fig. 1). The upper Ichinosawa is characterized by a deeply incised channel and steep slopes (40–65°). The channel gradient is mostly steeper than 25° and approaches the slope gradient of the talus slope (37.3°) in the uppermost part of the channel. Rockfall and dry ravel promoted by freeze-thaw in the winter and early spring are the predominant sediment infilling processes [11]. A large volume of sediment, ranging from sand particles to boulders, is stored in the channel bed and talus cones. The lower Ichinosawa is a debris flow fan, and the channel gradient is in the range of 15–20°.

* Corresponding author: imaizumi@shizuoka.ac.jp

© The Authors, published by EDP Sciences. This is an open access article distributed under the terms of the Creative Commons Attribution License 4.0 (https://creativecommons.org/licenses/by/4.0/).

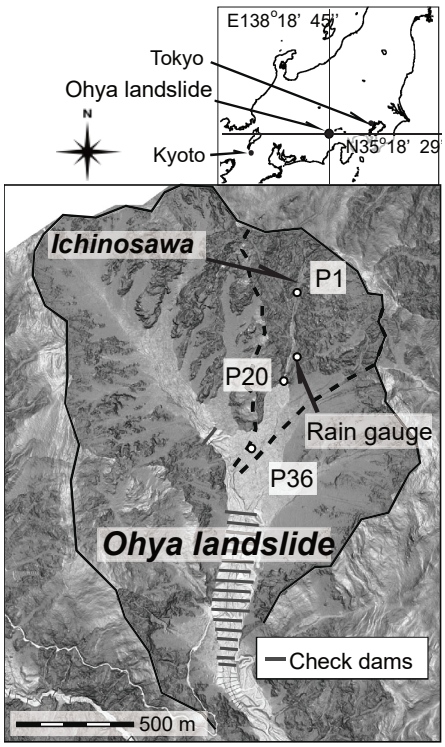

Fig. 1. Map of the Ohya landslide.

3 Methodology

3.1 Time lapse photography

In April 2020, twenty-seven time-lapse cameras (TLCs, Brinno TLC200Pro and TLC2000) were installed along the Ichinosawa torrent (P1–P36 in Fig. 1) to capture debris flows from the initiation zone to the deposition zone. The interval of images captured, which ranged from 1 to 10 s, differed among the cameras and periods. The number of TLCs was reduced to twenty-one in April 2021. A video camera was also installed at P20 in 2021.

We set 36 analysis points (P1 to P36) along the main channel of Ichinosawa with a spacing of approximately 20 m to interpret the arrival timing of debris flow surges using TLC images. Temporal changes in the flow type (partially and fully saturated flow) during debris flow events were visually and manually identified from images based on the presence of interstitial water on the flow surface [4]. The fully saturated flows are turbulent and are characterized by a black surface due to high concentrations of silty sediment in the interstitial water filling the boulder matrix. In contrast, muddy water is not identified in the flow surface matrix of the partially saturated flows (Fig. 2).

3.2 Pore water pressure

Pore water pressure sensors (KELLER AG für Druckmesstechnik, PR-26Y), which measure pressure in the range from 0 to 98 kPa with an accuracy of ±0.25%, were installed at two channel bank heights (S_1 and S_2 at 0 and 0.33 m from channel bed, respectively) with bedrock exposure at P20 in May 2020 (Fig. 3). Sensors were installed in holes made using a hammer drill and covered with a mortar. Three additional pressure sensors were installed at three heights (S_3, S_4, and S_5 at 0.64, 0.91, and 1.17 m from the channel bed, respectively) along the same cross-sectional line in May 2021. The data sampling interval was set at 4 s.

Components of the pore water pressure p are expressed as follows:

$$p = p_h + p_e = p_w + p_s + p_e \quad (1)$$

where p_h is the static water pressure, p_e is the excess pore water pressure, p_w is the static pressure of clean water, and p_s is the static pressure of suspended fine sediments. In the case of clean water without any p_e, $\partial p/\partial z$ is 9800 (Pa m^{-1}). Assuming that the maximum volumetric weight of the interstitial water is the same as that of the sediment (=2,650 kg m^{-3}), the maximum value of $\partial p_h/\partial z$ is 25,970 Pa m^{-1}. Therefore, excess pore water pressure certainly exists in debris flows if the $\partial p/\partial z$ exceeds 25,970 Pa m^{-1}. In this study, $\Delta p/\Delta z$, obtained from the difference in the pore water and elevation between the two water pressure sensors, was used as a substitute for $\partial p/\partial z$.

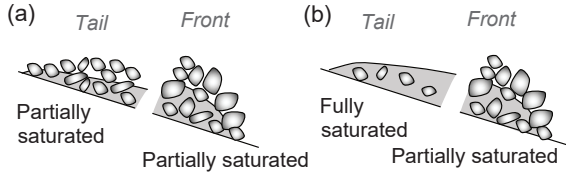

Fig. 2. Schematic diagram of surges including partially saturated flow [10]. (a) Surges in which only partially saturated flow was identified. (b) Surges in which both partially and fully saturated flows were identified.

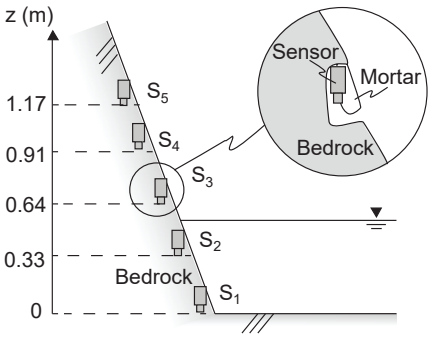

Fig. 3. Schematic diagram of water pressure sensors at P20.

4 Results

4.1 Debris flow on July 6, 2020

The debris flow was triggered by long-lasting rainfall from July 5 to July 11, 2020 (Fig. 4). The volume of sediment storage in the upper Ichinosawa, which was estimated by UAV-SfM (structure from motion using an unmanned aerial vehicle) [10], was 50,438 m^3 before the debris flow event. Debris flow surges first occurred at the upper end of the monitoring section at 10:24 on July 6. The peak rainfall intensity of the rainfall event was 7.6 mm/10 min recorded at 10:25 (Fig. 4a). The cumulative rainfall before this rainfall peak was 99.6 mm. A total of 65 surges were monitored by TLCs on

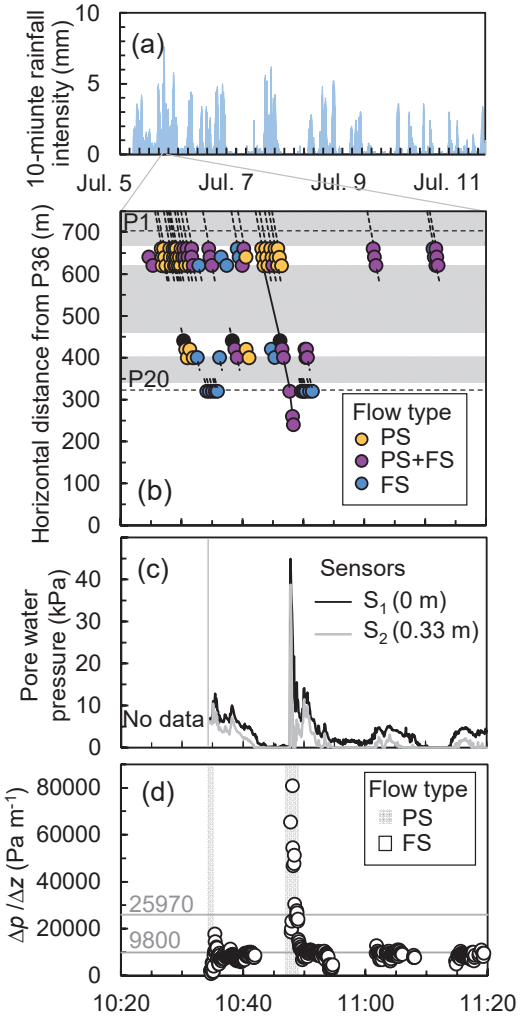

Fig. 4. Monitoring results of debris flow on July 6, 2020. (a) Rainfall intensity. (b) Runout timing and flow type at analysis points. Debris flow could not be monitored in gray sections because of shade of topography. PS and FS indicate partially and fully saturated flows, respectively. (c) Pore water pressure at P20. (d) $\Delta \boldsymbol{p}/\Delta \boldsymbol{z}$ calculated from S_1 and S_4 sensors.

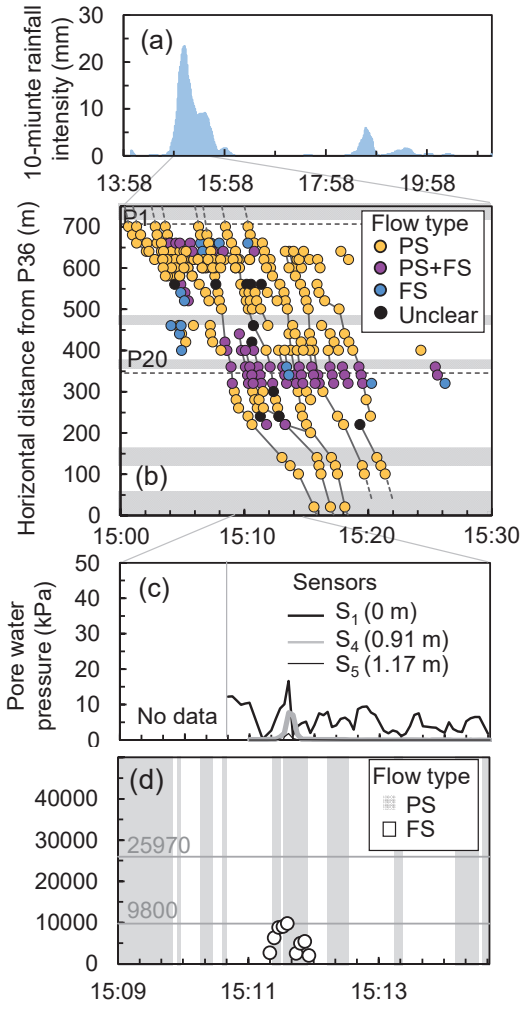

Fig. 5. Monitoring results of debris flow on July 13, 2021. (a) Rainfall intensity. (b) Runout timing and flow type at analysis points. Debris flow could not be monitored in gray sections because of shade of topography. PS and FS indicate partially and fully saturated flows, respectively. (c) Pore water pressure at P20. (d) $\Delta \boldsymbol{p}/\Delta \boldsymbol{z}$ calculated from S_1 and S_4 sensors.

July 6. Many surges during this event were initiated above P1 (Fig. 4b). Debris flow surges that started in the monitoring section of the TLCs (i.e., P1 to P20) were triggered by the erosion of channel deposits by overland flow and water and sediment supply from tributaries. Many of the surges were partially saturated flow, followed by a fully saturated flow (Fig. 2b). The debris flow passed P20 from 10:34 to 10:53 on July 6. The largest surge during this rainfall was monitored using a TLC at P20 from 10:47. The estimated peak flow height of this surge is 2.7 m. The pore water pressure sharply increased with the arrival of the surge (Fig. 4c). The first half of this surge was a partially saturated flow followed by a fully saturated flow. The Δp /Δz in the partially saturated flow exceeded the maximum value of $\partial p_h/\partial z$ (25,970 Pa m^{-1}), indicating a large excess pore water pressure in this surge (Fig. 4d); its travel distance was the longest among the surges during the rainfall event. The surge proceeded with a gentle channel section between P21 and P26, with a slope gradient of 15° to 20°.

4.2 Debris flow on July 13, 2021

Debris flow was triggered by a short and intensive rainfall with peak intensity of 23.4 mm/10 min on July 13, 2021 (Fig. 5a). The cumulative rainfall before this peak was 33 mm. The volume of channel storage in upper Ichinosawa before the debris flow event was 59,731 m^3. A total of 71 debris flow surges were detected using TLCs. Two sensors (S_2 and S_3) failed to observe this debris flow due to mechanical problems. Partially saturated debris flow was the predominant flow type during this event (Fig. 6). Many debris-flow surges were initiated in the channel section between P1 and P20 (Fig. 5b). Three debris flow initiation mechanisms were captured by the TLCs: erosion by overland flow proceeding over unsaturated deposits, sliding of channel deposits, and sediment and water supply from the channel bank, talus slope, and tributaries. Ten debris flow surges passed the P20 and reached the alluvial fan in lower Ichinosawa. The pore water pressure of the partially saturated flow at 15:11 was monitored using

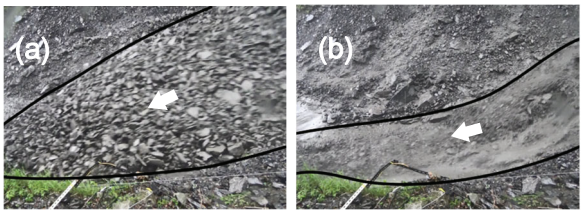

Fig. 6. Video camera images of (a) partially and (b) fully saturated flows captured at P20 on July 13, 2021. Black lines indicate sides of flows

three water pressure sensors (S_1, S_4, and S_5; Fig. 5c). The peak flow height was 1.2 m. $\Delta p / \Delta z$ was similar to or smaller than that of the static water pressure of clean water (9,800 Pa m^{-1}; Fig. 5d), indicating that unsaturated layers existed in the flow. The small $\Delta p / \Delta z$ value also implies low excess pore water pressure in the flow. We could not obtain $\Delta p / \Delta z$ in the other surges because a positive water pressure was not observed by S_4 owing to the small flow height.

5 Discussions

Debris flow surges on July 6, 2020, and July 13, 2021, were initiated by a series of mass movements in the initiation zone of debris flow (Figs. 4b and 5b). Most of the debris flow surges on July 6, 2020, occurred above P1, whereas many debris flow surges occurred between P1 and P20 on July 13, 2021. Because the cumulative rainfall on July 13, 2021, was less than that on July 6, 2020, a larger catchment area was likely needed for the occurrence of mass movements on July 13, 2021.

Both partially and fully saturated flows composed debris flow surges were observed on July 6, 2020, whereas partially saturated flow was the primary flow type on July 13, 2021. Debris flow monitoring in other torrents found that rainfall pattern is an important factor influencing flow type [3, 11]. The water content in channel deposits on July 13, 2021, was likely less than that on July 6, 2020, due to small antecedent rainfall before the rainfall peak, resulting in the occurrence of dry partially saturated debris flow surges.

The monitoring result of pore water pressure on July 6, 2020, implies that the partially saturated flow had a high excess pore water pressure (Fig. 4c). Although a partially saturated sediment mass can travel only in steep channel sections (>22.2° in Ichinosawa) in the context of static force [4], partially saturated flows have been monitored even in gentler channel sections [1, 2]. Decreasing the effective stress owing to the generation of excess pore water pressure likely increases the mobility of the unsaturated flow.

The difference in $\Delta p / \Delta z$ between the two debris flow events implies that the magnitude of excess pore water pressure varies among debris flow events (Figs. 4d, 5d). The dry flow condition on July 13, 2021, may have resulted in a small magnitude of excess pore water pressure. The difference in flow height between the two debris flow events also affects the difference in excess pore water pressure.

The volume of debris flow material is another factor that controls the debris flow characteristics [4, 12]. Because the volume of sediment storage was similar between July 6, 2020, and July 13, 2021 (50,438 and 59,731 m^3, respectively), the rainfall pattern was possibly a more important factor affecting the difference in the initiation and flow characteristics of the two debris flow events.

6 Summary and conclusions

To clarify the initiation and runout characteristics of partially saturated debris flows, we conducted a field monitoring experiment in the Ohya landslide scar. Three initiation mechanisms of debris flow surges were captured by the TLCs: erosion by overland flow proceeding over unsaturated deposits, sliding of channel deposits, and sediment and water supply from tributaries. The excess pore water pressure observed on July 6, 2020, likely increased the mobility of the partially saturated debris flows. The rainfall pattern controlled the initiation points of debris flow surges, the dominance of partially saturated flow, and the magnitude of excess pore water pressure.

Several factors, such as rainfall pattern, flow height, and volume of erosible sediments, can potentially affect the mobility of partially saturated debris flows. Consequently, the accumulation of monitoring data under various conditions is critical to enhance the understanding of partially saturated debris flows.

References

1. B. W. McArdell, P. Bartelt, J. Kowalski, Geophys. Res Lett. **34**, L07406 (2007)
2. S.W. McCoy, G. E. Tucker, J. W. Kean, J. A. Coe, J. Geophys. Res. **118**, 589–602 (2013)
3. K. Okano, H. Suwa, T. Kanno, Geomorphology **136**, 88–94 (2012)
4. F. Imaizumi, Y. S. Hayakawa, N. Hotta, H. Tsunetaka, O. Ohsaka, S. Tsuchiya, Nat. Hazards Earth Syst. Sci. **17**, 1923–1938 (2017)
5. R. M. Iverson, Rev. Geophys. **35**, 245–296 (1997)
6. M. A. Hampton, J. Sediment. Petrol. **49**, 753–758 (1979)
7. R. Kaitna, M. C. Palucis, B. Yohannes, K. M. Hill, W. E. Dietrich, J. Geophys. Res. Earth Surf. **121**, 415–441 (2016)
8. R. Zenit, M. L. Hunt, J. Fluid Mech. **375**, 345–361 (1998)
9. F. Imaizumi, R. C. Sidle, S. Tsuchiya, O. Ohsaka, Geophys. Res. Lett. **33**, L10404 (2006)
10. F. Imaizumi, T. Masui, Y. Yokota, H. Tsunetaka, Y. S. Hayakawa, Y. Hotta, Geomorphology **339**, 58–69 (2019)
11. M. Hürlimann, M, C. Abancó, J. Moya, I. Vilajosana, Landslides **11**, 939–953 (2014)
12. C. Gregoretti, M. Degetto, M. Bernard, G. Crucil, A. Pimazzoni, G. De Vido, M. Berti, A. Simoni, S. Lanzoni, Water Resour. Res. **52**, 8138–8158 (2016)